

Research Article

Experimental Study on Two-Step Concrete Corbels with Several Interface Conditions

Mohamed A. Hassan , M. Nasser Darwish, Said M. Allam , and Muhammad A. Diab 

Department of Structural Engineering, Faculty of Engineering, Alexandria University, Alexandria, Egypt

Correspondence should be addressed to Mohamed A. Hassan; mohamed.abdelhady12@alexu.edu.eg

Received 6 July 2023; Revised 21 October 2023; Accepted 30 October 2023; Published 23 November 2023

Academic Editor: Roberto Nascimbene

Copyright © 2023 Mohamed A. Hassan et al. This is an open access article distributed under the Creative Commons Attribution License, which permits unrestricted use, distribution, and reproduction in any medium, provided the original work is properly cited.

Corbels are usually used in precast concrete structures for beam–column connections and are common in industrial structures to support crane girders and may be required in new alteration works. To overcome the difficulty of casting columns with corbels, especially in precast concrete industry, columns are sometimes cast without their corbels, and then corbels are cast in a following step. Sometimes, new corbels get added to existing columns to support new crane girders. Thus, two-step corbels may be installed using different techniques depending on several criteria, and several factors affect their behavior, some of which mainly the interface conditions are experimentally investigated. One control specimen with a monolithic corbel and five two-step corbel specimens were tested. The mean roughness depth of the column–corbel interface varied between 4 and 8 mm. Moreover, using adhesive components on the hardened column–corbel interface was investigated. Besides, steel reinforcement implantation was attempted and studied for corbels with or without horizontal stirrups. For the tested cases, results show that two-step corbels can be a good replacement to monolithic corbels and can achieve up to 92% of the monolithic corbels capacity. Increasing the mean roughness interface depth between corbels and column slightly increased the two-step corbel capacity and improved its behavior. Using adhesive epoxy to the column–corbel interface can achieve the behavior and ultimate load capacity of two-step corbel with mean roughness depth of 4 mm. Implanting corbels' reinforcement is not recommended unless specific precautions and measures are assured and the embedment depth should be calculated and implemented to accommodate all expected failure mechanisms.

1. Introduction

Reinforced concrete (RC) corbels are common in concrete construction and are often used in precast structures and industrial buildings with overhead crane girders [1]. It is typically a short structural member that cantilevers out from a wall or a column to support a load [2]. According to some codes, the shear span-to-depth ratio of corbel is less than unity [2, 3]. Several definitions of corbels, short cantilevers, and ledge beams are available in literature [2, 4]. Experiments on concrete corbels were carried out previously by researchers to study their structural performance [5–12].

Corbels are monolithic in most of the previous studies, that is, when corbel and column are cast together in one step and all of the longitudinal and transverse reinforcement was previously installed in the form before concrete casting. Several researchers [13–19] used other types of corbels such as column insert, hidden corbel, and two-step corbel. Column

insert type is when a steel section (e.g., square hollow section, rolled channel, or a narrow plate) is inserted in the column to act as a corbel [13]. Hidden corbel is when an insert plate is cast into the column and a steel corbel gets attached to it either by welding or bolts later [14, 15]. In two-step corbel systems, corbels can be cast in a following step or time to column casting [16]. Transfer of forces between surfaces can be by means of grouted joints, shear keys, anchors mechanical connectors, steel reinforcement, reinforcing topping, or a combination [2]. Two-step corbels are used for several reasons, including decreasing the high production cost of precast columns with corbels and time. Regarding longitudinal steel reinforcement and horizontal stirrups, they may be bent inside the form work, then after removing columns from the form work, steel reinforcement can be inserted in the corbel forms. Other studies [17–19] inserted fully anchored threaded couplers in the columns, and the second-step corbel reinforcement was connected to such couplers. In some cases

when there is a need to install a new corbel to an existing column, the new corbel's longitudinal and transverse reinforcement is implanted by drilling and epoxying the reinforcement bars with specific embedment depth. The recommended embedment depth usually follows the epoxy manufacturer manuals, however, provided that these recommended embedment lengths must accommodate for all possible failure mechanisms and not just the pullout strength. Thus, further studies may be highly required, and the current research in an attempt is such direction.

In a two-step corbel, column–corbel-hardened interface should be treated with care in order to provide efficient shear friction capacity that can transfer the loading from the corbel to the column without failing. In designing for shear strength of concrete corbels, many existing design codes such as ACI [2] and Egyptian code [3] use mainly the “shear-friction theory” and/or the “strut-and-tie method” to predict shear strength. According to the shear friction concept, the shear strength of corbels is influenced by the coefficient of shear friction (μ), which ranges generally from 0.5 to 1.4 [2, 3] depending on the interface condition of existing RC members with the new concrete layer and the connection between precast members with cast-in-place parts and the used code. In the shear friction method, it is sometimes assumed [2] that all the shear resistance is due to the friction between the crack surfaces, and, hence, “artificial” high values of the friction coefficients may be required in the shear friction equations, so that the calculated shear strength will be in reasonable agreement with test results [2]. ECP [3] assumes that the shear concrete resistance is ignored, and the entire shear force is transferred by steel reinforcement crossing the interface. Such reinforcement is supposed to have adequate bond and embedment length to yield [2, 3].

Abundant studies have been conducted to explore the shear performance of RC corbels [20–23]. The bond strength of the interface is controlled by several parameters such as the substrate roughness degree, curing conditions, material strength and stiffness of both concrete layers, and the implanted steel reinforcement crossing the interface and its anchorage [17, 24–27]. The concerns related to such issue are not only related to static loading, but also the dynamic loads and several precasting conditions can critically generate adverse and noncontributable stresses on such RC element [28–30].

Although several researches have carried out to investigate shear in concrete corbels, very limited studies focused on exploring the impact of several parameters on the column–corbel interface surface in particular with the case of two-step corbels considering separation mode. An experimental investigation has been carried out to explore the performance of the column–corbel interface surface. The selected factors to be exploited were: varying the mean surface roughness depths using epoxy adhesive along with the presence of steel reinforcement. Test results are analyzed and discussed in terms of load–deflection response, cracking and ultimate load capacity, steel load–strain developments, crack pattern, and failure mode for the all tested corbels.

2. Experimental Program

An experimental study was carried out to study the behavior of RC two-step concrete corbels subjected to vertical monotonic loads. Six RC specimens (M1, M2, M3, M4, M5, and M6) were tested up to failure. The height of the square column was 800 mm with a side length of 200 mm supporting two corbels in opposite directions, as shown in Figure 1. The width, depth, and length of each corbel were 200, 300, and 300 mm, respectively. Figure 1 shows the dimensions and loading for all the corbels and columns. Specimen M1 was taken as the control specimen, where both column and corbels were cast monolithically at the same time. Specimens M1, M2, M3, and M4 had the same dimensions and reinforcement and varied only in the interface surface condition. Specimen M2 was prepared in two steps. In the first-step column, concrete only was cast and corbel reinforcement was already installed inside the form, then the interface between the column and corbels was roughened by using a power impact driller/hammer to achieve a chosen mean roughness depth of 4 mm, and corbel steel reinforcement was prepared, as shown in Figure 2(a). In the second step, concrete for the corbels was cast after 7 days of casting the concrete column. Specimen M3 was cast in the same steps as specimen M2, but only differed in the mean depth of roughness of the column interface surface, which was made equal to 8 mm, as shown in Figure 2(b). It can be mentioned that interface roughness of specimens has been captured with similar previous recommendation [18, 31]. Specimen M4 was prepared in the same way as specimen M2 but epoxy-based adhesive was applied between the concrete columns without applying any surface roughening, as shown in Figure 3. For specimen M5, the column's concrete was cast in the first step without installing any of the corbel reinforcement, then corbel reinforcement and horizontal corbel stirrups were implanted using adhesive epoxy, following some recommended steps of the used implanting adhesive (e.g., embedment length = 8 times the bar diameter), as shown in Figure 4. In specimen M6, similar procedures such as those for specimen M5 were applied but only the main reinforcement was implanted, as shown in Figure 5. For specimens M5 and M6, the interface between the corbel and column was painted using adhesive epoxy-based component.

For all test specimens, upper and lower main steel in the corbels, vertical stirrups, horizontal stirrups (except M6), and column reinforcement were all kept constant. In addition, the web reinforcement was closed stirrups. For specimens M1, M2, M3, and M4, the main longitudinal reinforcements were extended to the full length of the specimen and through the depth to provide sufficient anchorage, as shown in Figure 1. The clear concrete cover was 25 mm. The concrete compressive strength (f_{cu}) was selected from three concrete cubes with dimensions of 150 mm × 150 mm × 150 mm respecting to the Egyptian code specification [3]. Table 1 presents f_{cu} values and geometry details of the tested specimens.

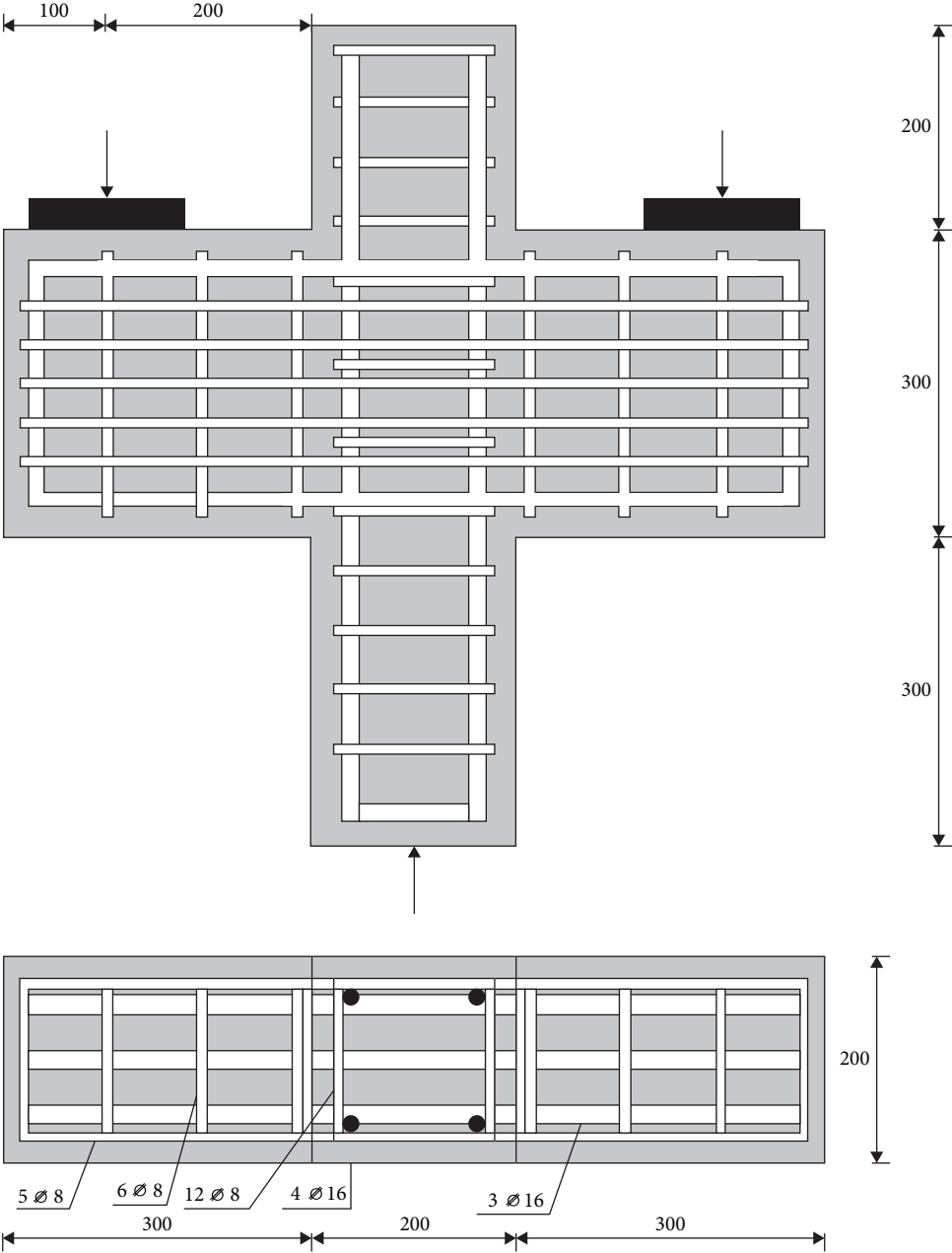


FIGURE 1: Reinforcement and geometric details of the tested corbel with respect to ECP [3] (units in mm).

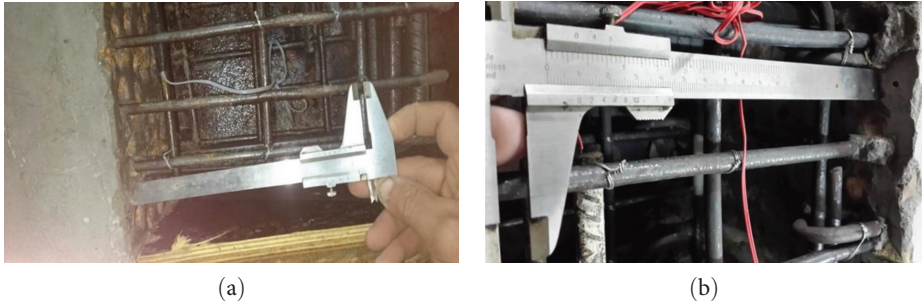


FIGURE 2: Interface roughness of tested specimens: (a) M2 and (b) M3.



FIGURE 3: Interface between corbel and column painted using adhesive epoxy-based component in specimen M4 (*photo rotated 90° for clarification*).



(a)



(b)

FIGURE 4: Main steel and stirrups implanted into the column tested specimen M5 (*photo rotated 90° for clarification*).



(a)



(b)

FIGURE 5: Main steel implanted into the column of tested specimen M6 (*photo rotated 90° for clarification*).

3. Material Properties

The normal strength concrete used in the present tests consisted of Ordinary Portland Cement, natural siliceous sand, crushed limestone with 12.7 mm maximum nominal size, and water. The mix proportions of cement, natural siliceous sand, and crushed limestone by weight were 1 : 1.6 : 2.6. The water-to-cementitious materials (w/c) ratio was 0.44. Concrete cubes (150 mm) were tested after 28 days, and the average compressive cube strength value was 32 MPa. Two kinds of steel reinforcement were used. Deformed bars of 16 mm diameter were used as tension reinforcement in corbels and as compressive reinforcement in columns, whereas plain bars of 8 mm diameter were used for vertical and horizontal stirrups for both corbels and columns. The material properties of steel bars were measured from tensile tests, and it was found that the yield stress of the 16 and 8 mm diameter bars was measured as 360 and 280 MPa, respectively, whereas the tensile strength was measured as 560 and 450 MPa,

respectively. An epoxy-based component adhesive, commercially named X-Roc Epoxy Bond, was used as the bonding material at the interface of the corbel and column connections. This material was used for bonding between old hardened concrete cast earlier and the newly cast concrete. Several considerations were involved in applying adhesives effectively, including careful surface preparation such as removing the cement paste, grinding the surface by using a disk sander, removing the dust generated by surface grinding using an air blower, and careful curing, as these are critical for bond performance. The two components (white and black paste) of this epoxy material were mixed 5 : 1 by weight, according to manufacturer's recommendations.

4. Experimental Setup

The specimens were tested after 28 days of concrete casting. Two days prior to testing, the corbels were painted white to help in identifying the cracks during tests. A universal testing

TABLE 1: Summary of geometry and interface surface conditions of the tested specimens.

Specimen ID	Dimensions of the section of corbel ($b \times h$) (mm)	f_{cu} (MPa)	Interface surface condition
M1	200 × 300	32	Control, monolithically
M2			Contact surface mean roughness depth = 4 mm
M3			Contact surface mean roughness depth = 8 mm
M4			Using epoxy adhesive without surface roughness
M5			Implanted main steel reinforcement and vertical stirrups
M6			Implanted main steel reinforcement only

Note. b , width of corbel; h , height of corbel.

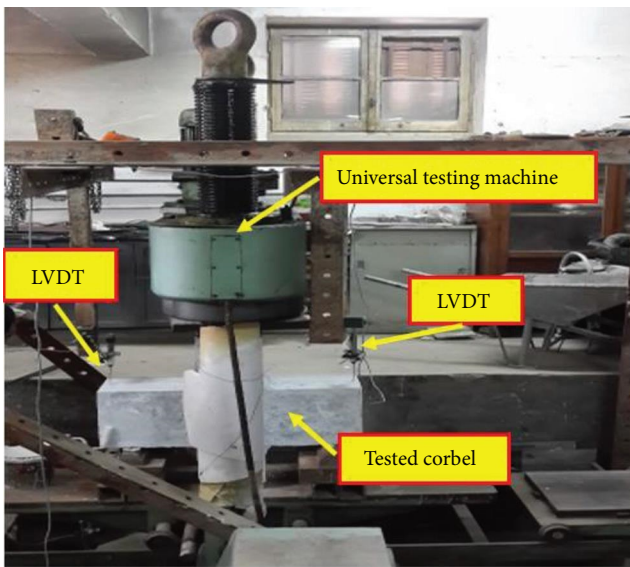


FIGURE 6: Typical test setup of tested specimens.

machine with a capacity of 3,000 kN was used for testing the specimens. The test setup of a typical specimen is shown in Figure 6. The specimen was leveled on two hinged supports, and hydraulic jack was employed to loading corbels at shear span of 200 mm producing shear span-to-depth ratio (a/d) equal to 0.74 (less than 1.00) considering the code recommendation [3]. The specimens were tested in an inverted position; the vertical load was applied to the column, while the hydraulic jack transferred the load to the corbels through hinges, as shown in Figures 6 and 7. Each corbel was loaded on a 200 mm × 120 mm × 10 mm steel plate. Four linear variable differential transformers (LVDTs) were placed to measure the deflection, whereas four strain gauges were used to measure the strain distributions of the main steel reinforcement bars. The positions of strain gauges in the tested specimens are shown in Figure 7. The load was increased by an increment of 25 kN, and the duration of each increment was about 5 min. At each loading increment, deflection and steel strains were recorded, and crack pattern was indicated until failure took place.

5. Results and Discussion

5.1. Failure Modes and Crack Patterns. Corbels may fail in several ways, including shearing along the interface between the column and the corbel, crushing or splitting of the compression strut, yielding of the tension tie, besides other kinds of failure (not in the cases studied), including localized bearing or shearing failure under the loading plates. Figure 8 shows the failure modes and crack patterns of the tested specimens. Failure of specimens M1, M2, M3, and M4 was by crushing of diagonal compression strut accompanied by splitting cracks. Using two-step corbels with previously installed reinforcement in the columns (M2 to M4) did not change the failure pattern for (a/d) equal to 0.74, and no slippage at the column–corbel interface was observed during loading. Specimens M5 and M6 failed by early pullout failure and slippage of the implanted reinforcement, causing premature failure.

For the control specimen M1, a diagonal hair crack appeared at the shear zone at a load of 125 kN (about 29% of $P_u = 437$ kN, where P_u is the recorded test failure load). In addition, at a load of 250 kN (about 57% of P_u), a vertical flexural crack appeared at the column face (interface surface between column and corbel). As the load was increased, the width of the diagonal crack gradually increased and extended downward to the loading point and upward to the column–corbel interface. Flexure crack depth extends vertically to only 17% of corbel depth at failure. Before the failure of specimen M1, additional diagonal cracks parallel to the main diagonal crack appeared at the tensile side just after main reinforcement yielding ($P_y = 400$ kN). The corbel at both sides showed nearly the same behavior until just before failure. Failure occurred at one side at a load of $P_u = 437$ kN, as shown in Figure 8(a). The failure can be classified as crushing of the compression strut (shear failure). For specimen M2, as shown in Figure 8(b), a diagonal hair crack appeared at the shear zone at a load of 75 kN (about 20% of $P_u = 375$ kN), whereas at a load of 200 kN (about 53% of P_u), a vertical flexural crack appeared at the column face (interface surface between column and corbel). As the load was increased, a similar behavior to that of specimen M1 was observed and failure was the same as M1 and can be classified as a shear failure. For specimen M3, as shown in Figure 8(c), a

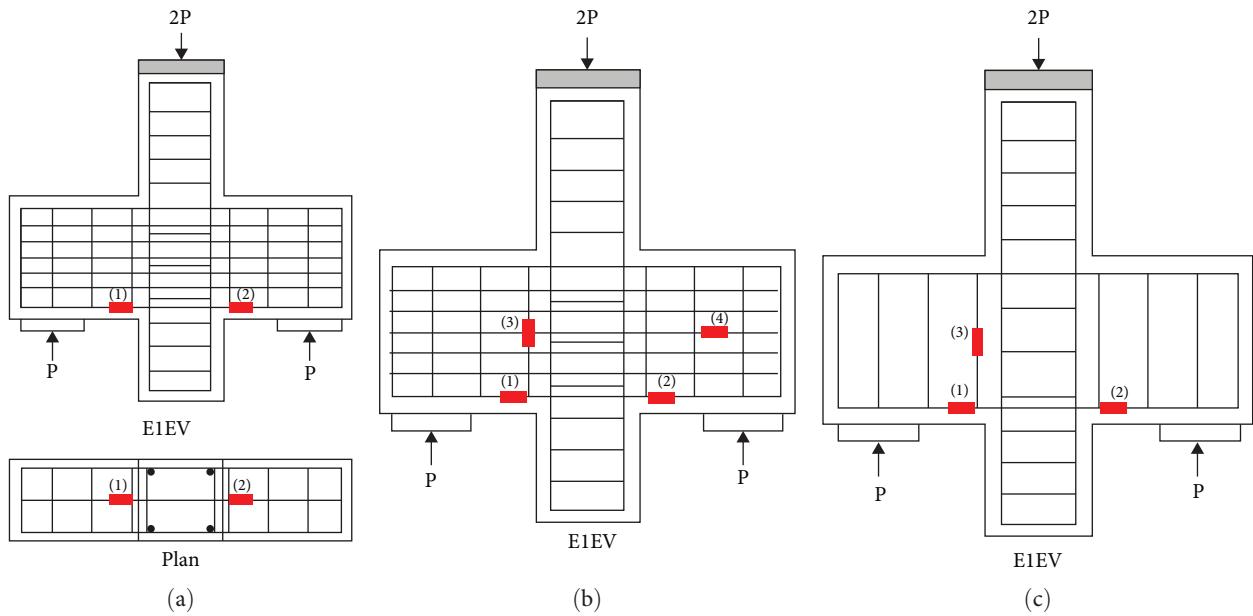


FIGURE 7: Positions of strain gauges in the tested specimens: (a) M1 and M2; (b) M3, M4, and M5; (c) M6.

diagonal hair-like crack appeared at the shear zone at a load of 100 kN (about 25% of $P_u = 400$ kN). The vertical flexural crack at the column face appeared at a load of 300 kN (about 75% of P_u), and the failure of the specimen occurred at a load of P_u of 400 kN. Failure of specimen M3 was the same as the other specimens M1 and M2 and can be classified as a shear failure. Failure of M4, as shown in Figure 8(d), was the same as the other three specimens (M1, M2, and M3), i.e., shear failure. The diagonal hair crack at specimen M4 appeared at the shear zone at a load of 100 kN (about 27% of $P_u = 375$ kN).

For specimens M5 and M6, as shown in Figures 8(d) and 8(f), respectively, no diagonal cracks appeared until failure (which was premature), as shown in Figure 8. A vertical crack appeared at the interface between the corbel and column at a load of 75 kN (about 75% of specimen premature failure load; $P_u = 100$ kN). Additional vertical cracks occurred at failure due to premature tension breakout failure of concrete surrounding the implanted bars at a load of 100 kN. The failure occurred by slippage of both the main steel and horizontal stirrups (in M5) and the main steel (in M6) from the column, causing separation of the corbel from the column due to insufficient anchorage length of the implanted steel reinforcement. The failure is classified as premature anchorage failure (breakout failure in tension).

5.2. Load–Strain Distributions. Figure 9 shows the recorded load–strain distributions of the tested specimens. For specimens M1 and M2, the maximum strain at ultimate load (P_u) was close to 0.003 (i.e., about 1.25 of ϵ_{yield}). For specimen M3, the yield of longitudinal tension steel occurred at a load of 370 kN (92.5% P_u). The reinforcement tensile strain at P_u was 0.0028. However, no yield was recorded for both horizontal and vertical stirrups. At P_u , the strain in horizontal stirrups (strain gauge no. 4) was 0.00125 (89% ϵ_{yield}), while in

vertical stirrups (strain gauge no. 3) at P_u , it was only 0.0005 (36% of ϵ_{yield}). For specimen M4, the yield of the longitudinal steel occurred at a load of 365 kN (97% P_u). The reinforcement tensile strain at P_u was 0.0027. Both horizontal and vertical stirrups did not reach yielding similar to M3. At P_u , the strain in horizontal stirrups (strain gauge no. 4) was only 0.00125 (89% ϵ_{yield}). For specimens M5 and M6, premature anchorage failure took place and, hence, naturally no yield occurred in tensile steel, as shown in Figures 8(e) and 8(f).

Hence, for the previous studied cases, two-step corbels with adequate steel anchorage (M2, M3, and M4) and monolithic corbel (M1) tend to fail due to diagonal compression strut failure and splitting just after the main longitudinal tensile reinforcement reaching its yield. The insufficient length of steel bars resulted in slippage premature failure which is not recommended for such cases; however, these bars presented yield stage followed by pulling out.

5.3. First Flexural Load, Diagonal Cracking Load, Yielding Load, and Ultimate Load. Table 2 shows first flexural cracking load, diagonal cracking load, yielding load, and ultimate load of the tested specimens. For the tested specimens (M2–M4), two-step corbels showed that it can be a good replacement to monolithic corbels. They could not achieve their full capacity but achieved from 86% to 91.5% of monolithic corbel (M1) ultimate load. Generally, two-step corbels (M2–M4) experienced earlier cracking than monolithic corbels (i.e., M1). Two-step corbels (M2–M4) had slightly lower ultimate strength than the monolithic corbel (M1) regardless of the mean roughness depth or the used adhesion elements at the column–corbel interface. Using the recommended embedment depth of implanted reinforcement (eight times the bar diameter) (as applied in M5 and M6) was not



FIGURE 8: Failure modes of the tested specimens (note tested in inverted position).

adequate nor enough to provide against inadequate breakout strength of the concrete surrounding the implanted bars (and, hence, for the implanted reinforcement to develop its yield strength and be effective); besides, it was not enough for the corbel shear strength to be achieved. Thus, premature anchorage failure occurred in specimens M5 and M6. Increasing the mean roughness depth (M2 and M3) increased the ultimate corbel strength. Also, using adhesive elements at column–corbel interface (M4) gave almost the same ultimate corbel strength of specimen M2 with mean roughness depth of 4 mm.

5.4. Load–Deflection Curves. Figure 10 shows the load–deflection relationship of the tested specimens. Extra deformation and some interface deformation occurred in the two-step corbels. Thus, the two-step corbels stiffness, as naturally expected, was less than that of the monolithic corbel (M1). Failure (M1–M4) occurred after main reinforcement yielding and at almost the same corbel deflection. Using

adhesive at column–corbel interface (M4) caused an average behavior between corbel M2 with mean roughness depth of 4 mm and corbel M3 with mean roughness depth of 8 mm.

5.5. General Discussion. For shear friction calculations, some codes, e.g., ECP [3] assume that concrete shear resistance is to be ignored and all shear to be transferred by steel reinforcement. For shear friction equations, the shear friction coefficient, u :

- (1) According to ECP [3]: $u = 1.2$ (monolithic construction), $u = 0.80$ (roughness depth about 6 mm), and $u = 0.50$ (roughness thickness < 6 mm or steel elements attached to concrete surface).
- (2) According to ACI [2] for normal strength concrete: $u = 1.4$ (monolithic construction), $u = 1.0$ (concrete placed against hardened concrete roughened to a full amplitude of ~ 6 mm), $u = 0.60$ (concrete placed

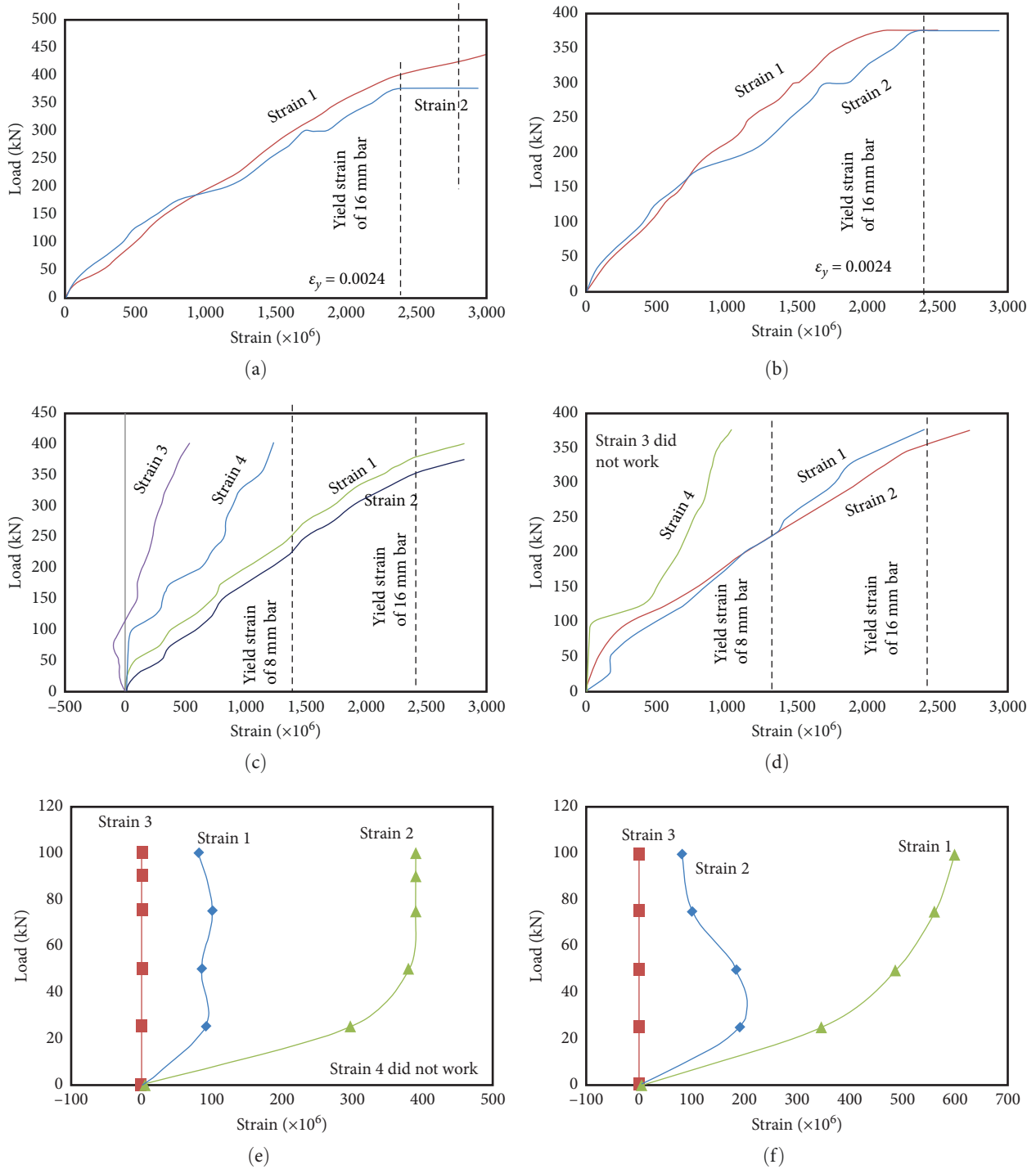


FIGURE 9: Strain distributions of the tested specimens: (a) M1; (b) M2; (c) M3; (d) M4; (e) M5; (f) M6.

against hardened concrete not intentionally roughened), and $u = 0.70$ (steel elements and with shear transferred across the contact surface by welded deformed bars).

The slight differences in test results for the ultimate load show that:

- (1) Specimen M2 with 4 mm mean surface roughness depth, achieved 85% of P_u of M1.

- (2) Specimen M3 with 8 mm mean roughness depth achieved 92% of P_u of M1.

- (3) Specimen M4 with epoxy adhesive without surface roughness achieved 85% of P_u of M1.

For the previous tested specimens, the differences in P_u for M1–M4 are not significant, indicating that the change in the mean roughness depth of the interface was not that effective, and the variation from 4 to 8 mm between M2 and M3 gave only a mere 7% increase in load capacity.

TABLE 2: Observed cracking and ultimate loads of the tested specimens.

Specimen ID	Cracking load (kN)		Yielding load (kN)		Ultimate load P_u (kN)	$\frac{P_{cr1}}{P_u}$	$\frac{P_{cr2}}{P_u}$	$\frac{P_y}{P_u}$	$\frac{P_u}{P_{u,M1}}$	Mode of failure
	Flexural crack (P_{cr1})	Diagonal crack (P_{cr2})	$P_{y,1}$	$P_{y,2}$						
M1	250	125	400	—	437	0.57	0.29	0.92	1	CCS
M2	200	75	325	—	375	0.53	0.20	0.87	0.86	CCS
M3	300	100	370	NY	400	0.75	0.25	0.85	0.92	CCS
M4	200	100	365	NY	375	0.53	0.27	0.97	0.86	CCS
M5	75	—	NY	NY	100PR	0.75	—	—	0.23PR	Premature breakout
M6	75	—	NY	NY	100PR	0.75	—	—	0.23PR	Premature breakout

Note. NY, steel not yielded; $P_{y,1}$, load at main steel; $P_{y,2}$, load at transverse steel; CCS, crushing of compression strut (shear failure); breakout failure in tension (anchorage failure); PR, premature failure.

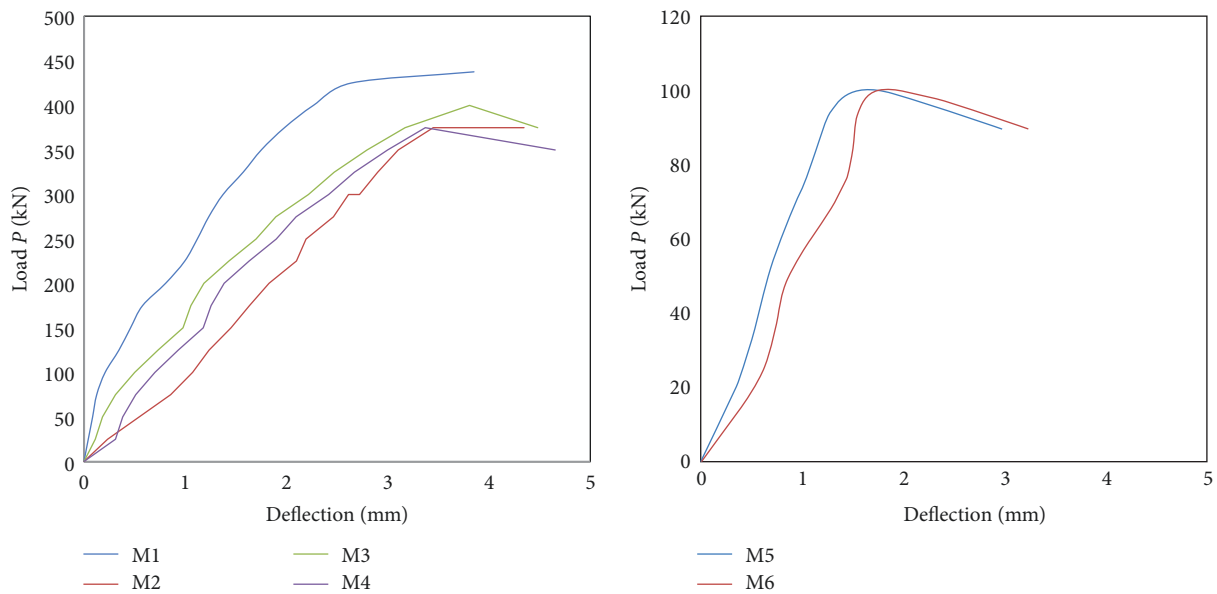


FIGURE 10: Load–deflection curves of tested specimens.

There are differences in the values of shear friction coefficients within codes and high scatter, and if code values were theoretically applied, then:

- (1) According to ECP [3]: The ultimate load of specimen M1 should have been much higher (1.5 times) than that of specimen M2 and higher (2.4 times) than that of specimen M3.
- (2) According to ACI [2]: The ultimate load of specimen M1 should have been the same or 1.4 times higher than that of specimen M3 and higher (more than two times) than that of specimen M2.

However, specimens M1, M2, and M3 experimentally showed only slight differences in results, which are not in accordance with theoretical ECP or ACI stipulations. Specimens M2 and M3 (with roughness depth 4 and 8 mm) should have had higher differences in results, according to both ECP [3] and ACI [2]; however, this was not the case. Unless the stipulated limiting value for surface roughness

depth of 6 mm in some codes [2, 3] is totally approximate. However, this is not new or strange and as previously stated [2] “artificial” high values of the friction coefficient are adopted in the shear friction equations. The estimation of the coefficient of friction and roughness depth seems not that sensitive to changes around the stipulated value of 6 mm. Besides, may be the tested specimens geometry with surface roughness depth 4 and 8 mm is too close to the stipulated approximate limit of the 6 mm value or other factors including the accuracy of measuring and estimating surface roughness, etc. However, on top of such factors may be the size effect. Besides, as it can be easily noted, the shear friction coefficients are different between codes and even within codes themselves.

Premature failures of specimens M5 and M6 confirm the need for adequate embedment length/anchorage for steel reinforcement crossing the shear plane on both sides of the shear plane to preclude premature slippage or breakout in tension and to ensure developing their yield strength. Hence, implanting corbels’ reinforcement is not recommended

unless specific precautions and measures are assured and the embedment depth should be calculated and implemented to accommodate for all expected failure mechanisms.

6. Conclusions

This paper presents experimental work on RC two-step and monolithic corbels with some different conditions of the column–corbel interface. In the tested specimens, concrete was cast either monolithically or by casting concrete against hardened concrete with different degrees of roughened surface area between the column and corbels. The effect of the addition of adhesive epoxy to the contact surface, as well as the effects of implanted main corbels steel reinforcement in the column with or without horizontal stirrups, was investigated. For the studied limited cases, the following can be noted:

- (1) Two-step corbels (M2–M4) can be a good replacement to monolithic corbels and can achieve up to 92% of monolithic corbels capacity with a slight reduction in corbel stiffness.
- (2) For (a/d) equal to 0.74, using two-step corbels with previously installed reinforcement in the columns (M2–M4), it did not change the failure mechanism of monolithic corbels (M1). Both of the two corbel types failed due to crushing of diagonal compression strut.
- (3) For (a/d) equal to 0.74, monolithic and two-step corbels (M1–M4) tend to fail just after yielding of their main reinforcement.
- (4) The roughness of the interface surface between the corbel and column (M2–M4) had only a slight effect on the ultimate capacity of the tested specimen when compared to monolithic corbel (M1). The ultimate load of M2 and M3, with mean surface roughness depth of 4 and 8 mm, respectively, was 14% and 8% lower than that of specimen M1. Increasing the mean roughness depth between corbels and column (comparing M2–M4) only slightly increased the two-step corbel capacity.
- (5) Using adhesive epoxy to the column–corbel interface in the two-step corbel with mean roughness depth of 4 mm (M4) could achieve the behavior and values near the ultimate load capacity of monolithic corbel (M1) with only a reduction of about 14%.
- (6) Using the recommended embedment depth of the implanting epoxy (M5 and M6) was not enough to provide adequate breakout strength of the implanted reinforcement bars crossing the interface causing premature failure of the corbel. Thus, implanting corbels reinforcement is not recommended unless specific precautions and measures are assured and the embedment depth should be calculated and implemented to accommodate for all expected failure mechanisms, including premature slippage (breakout in tension) and to ensure that the reinforcement crossing the interface develops yield.

Data Availability

All data and outcomes of the experimental results are presented in the manuscript.

Disclosure

This investigation forms a part of the ongoing Ph.D. research of the first author at the Faculty of Engineering, Alexandria University, Egypt.

Conflicts of Interest

The authors declare that they have no conflicts of interest.

Acknowledgments

The authors declare that all the payments have been done by themselves. The assistance of Prof. M.S. Shoukry and the help of the staff of the department's concrete laboratory are highly appreciated.

References

- [1] K. S. Abdul-Razzaq, A. A. Dawood, and A. H. Mohammed, "A review of previous studies on the reinforced concrete corbels," *IOP Conference Series: Materials Science and Engineering*, vol. 518, Article ID 022057, 2019.
- [2] ACI Committee, *ACI 318-19: Building Code Requirements for Structural Concrete and Commentary*, American Concrete Institute, Farmington Hills, Michigan, USA, 2019.
- [3] National Housing and Building Research Council, *ECP 203-2020/2021: Egyptian Code for Design and Construction of RC Buildings*, HBRC, Cairo, Egypt, 2021.
- [4] M. N. Darwish, "Shear in high strength concrete corbels," in *Proceedings of the Eighth Arab Structural Engineering Conference*, vol. 2, pp. 747–760, Cairo University, Cairo, Egypt, October 2000.
- [5] S. J. Foster, R. E. Powell, and H. S. Selim, "Performance of high-strength concrete corbels," *ACI Structural Journal*, vol. 93, no. 5, pp. 555–563, 1996.
- [6] M. M. Ahmed, H. Diab, and A. A. M. Drar, "Shear behaviour of high strength fiber reinforced concrete corbels," *JES. Journal of Engineering Sciences*, vol. 40, no. 4, pp. 969–987, 2012.
- [7] J. Assih, I. Ivanova, D. Dontchev, and A. Li, "Concrete damaged analysis in strengthened corbel by external bonded carbon fibre fabrics," *Applied Adhesion Science*, vol. 3, Article ID 21, 2015.
- [8] M. Lachowicz and K. Nagrodzka-Godycka, "Experimental study of the post tensioned prestressed concrete corbels," *Engineering Structures*, vol. 108, pp. 1–11, 2016.
- [9] T. Urban and Ł. Krawczyk, "Strengthening corbels using post-installed threaded rods," *Structural Concrete*, vol. 18, no. 2, pp. 303–315, 2017.
- [10] G. Campione, L. La Mendola, and M. Papia, "Flexural behaviour of concrete corbels containing steel fibers or wrapped with FRP sheets," *Materials and Structures*, vol. 38, pp. 617–625, 2005.
- [11] N. I. Fattuhi, "Reinforced corbels made with plain and fibrous concretes," *ACI Structural Journal*, vol. 91, no. 5, pp. 530–536, 1994.

- [12] P. R. Chakrabarti, D. J. Farahi, and S. I. Kashou, "Reinforced and precompressed concrete corbels—an experimental study," *ACI Structural Journal*, vol. 86, no. 4, pp. 405–412, 1989.
- [13] K. S. Elliott, *Precast Concrete Structures*, Taylor & Francis, CRC Press, Boca Raton, 2nd edition, 2017.
- [14] Peikko Group Corporation, *PCs® Corbel—Hidden Corbel for Supporting Beams*, Peikko Group, Technical Manual, 2019.
- [15] P. Kyriakopoulos, S. Peltonen, I. Vayas, C. Spyarakos, and M. V. Leskela, "Experimental and numerical investigation of the flexural behavior of shallow floor composite beams," *Engineering Structures*, vol. 231, Article ID 111734, 2021.
- [16] M. K. el Debs and J. B. A. Costa, "High performance concrete corbels cast in different stages of the column," *Concrete Plant International*, vol. 5, pp. 174–181, 2010.
- [17] D. de Lima Araújo, E. M. de Oliveira, E. M. O. Silva, S. A. Coelho, and M. K. El Debs, "Experimental analysis of a modified two-step corbel for precast concrete system," *Engineering Structures*, vol. 242, Article ID 112585, 2021.
- [18] D. L. de Araújo, S. A. Coelho, S. R. M. de Almeida, and M. K. El Debs, "Computational modelling and analytical model for two-step corbel for precast concrete system," *Engineering Structures*, vol. 244, Article ID 112699, 2021.
- [19] Y. M. Neuberger and D. de Lima Araújo, "An improved analytical model for two-step corbels in a precast concrete system," *Engineering Structures*, vol. 284, Article ID 115947, 2023.
- [20] A. H. Mattock, "Shear transfer in concrete having reinforcement at an angle to the shear plane," *ACI Symposium Volumes*, vol. 42, pp. 17–42, 1974.
- [21] A. H. Mattock, "Shear friction and high-strength concrete," *ACI Structural Journal*, vol. 98, no. 1, pp. 50–59, 2001.
- [22] A. H. Mattock and N. M. Hawkins, "Shear transfer in reinforced concrete—recent research," *PCI Journal*, vol. 17, no. 2, pp. 55–75, 1972.
- [23] A. H. Mattock, L. Johal, and H. C. Chow, "Shear transfer in reinforced concrete with moment or tension acting across the shear plane," *PCI Journal*, vol. 20, no. 4, pp. 76–93, 1975.
- [24] K. Krc, S. Wermager, L. H. Sneed, and D. Meinheit, "Examination of the effective coefficient of friction for shear friction design," *PCI Journal*, vol. 61, no. 6, pp. 44–67, 2016.
- [25] R. T. Morgan, "Shear friction design using ACI 319-19 anchoring to concrete provisions for post installed reinforcing bar design," *Ask Hilti*, 2023.
- [26] A. Hamoda, M. Emara, F. Abdelazeem, and M. Ahmed, "Experimental and numerical analysis of RC beams strengthened with ECC and stainless steel strips," *Magazine of Concrete Research*, vol. 75, no. 5, pp. 251–270, 2023.
- [27] A. Hamoda, G. Elsamak, M. Emara, M. Ahmed, and Q. Q. Liang, "Experimental and numerical studies of reinforced concrete beam-to-steel column composite joints subjected to torsional moment," *Engineering Structures*, vol. 275, Part A, Article ID 115219, 2023.
- [28] F. Cavalieri, D. Bellotti, and R. Nascimbene, "Seismic vulnerability of existing precast buildings with frictional beam-to-column connections, including treatment of epistemic uncertainty," *Bulletin of Earthquake Engineering*, vol. 21, pp. 1117–1138, 2023.
- [29] E. Brunesi, S. Peloso, R. Pinho, and R. Nascimbene, "Friction characterization testing of fabric felt material used in precast structures," *Structural Concrete*, vol. 21, no. 2, pp. 735–746, 2020.
- [30] W. M. Montaser, I. G. Shaaban, J. P. Rizzuto, A. H. Zaher, A. Rashad, and S. M. El Sadany, "Steel reinforced self-compacting concrete (SCC) cantilever beams: bond behaviour in poor condition zones," *International Journal of Concrete Structures and Materials*, vol. 17, Article ID 19, 2023.
- [31] S. K. Bandaru and D. R. Seshu, "An experimental study on the interface shear strength of reinforced geopolymer concrete corbels," *Australian Journal of Civil Engineering*, vol. 20, no. 2, pp. 359–373, 2022.